Acta Cryst E CRYSTALLOGRAPHIC COMMUNICATIONS

ISSN 2056-9890

Synthesis of FeN_4 at 180 GPa and its crystal structure from a submicron-sized grain

Maxim Bykov,[a]* Saiana Khandarkhaeva,[a] Timofey Fedotenko,[b] Pavel Sedmak,[c] Natalia Dubrovinskaia[b] and Leonid Dubrovinsky[a]

[a]Bayerisches Geoinstitut, University of Bayreuth, 95440 Bayreuth, Germany, [b]Material Physics and Technology at Extreme Conditions, Laboratory of Crystallography, University of Bayreuth, 95440 Bayreuth, Germany, and [c]European Synchrotron Radiation Facility, BP 220, 38043 Grenoble Cedex, France. *Correspondence e-mail: maks.byk@gmail.com

Received 7 August 2018
Accepted 28 August 2018

Edited by M. Weil, Vienna University of Technology, Austria

Keywords: polynitrides; iron tetranitride; high-pressure single-crystal X-ray diffraction; crystal structure.

CCDC reference: 1864279

Supporting information: this article has supporting information at journals.iucr.org/e

Iron tetranitride, FeN_4, was synthesized from the elements in a laser-heated diamond anvil cell at 180 (5) GPa and 2700 (200) K. Its crystal structure was determined based on single-crystal X-ray diffraction data collected from a submicron-sized grain at the synchrotron beamline ID11 of ESRF. The compound crystallizes in the triclinic space group $P\overline{1}$. In the asymmetric unit, the Fe atom occupies an inversion centre (Wyckoff position 1*d*), while two N atoms occupy general positions (2*i*). The structure is made up from edge-sharing [FeN_6] octahedra forming chains along [100] and being interconnected through N—N bridges. N atoms form *catena*-poly[tetraz-1-ene-1,4-diyl] anions $[-N{=}N-N-N-]_\infty^{2-}$ running along [001]. In comparison with the previously reported structure of FeN_4 at 135 GPa [Bykov *et al.* (2018). *Nat. Commun.* **9**, 2756], the crystal structure of FeN_4 at 180 GPa is similar but the structural model is significantly improved in terms of the precision of the bond lengths and angles.

1. Chemical context

Polynitrogen compounds have attracted great interest because of their potential applications as high-energy-density materials. Recently, a variety of nitrogen-rich compounds containing polymeric and oligomeric nitrogen chains, N_5 or N_6 rings, or even more complex networks have been predicted to be stable at high pressures (Steele & Oleynik, 2016, 2017; Zhang *et al.*, 2017; Xia *et al.*, 2018). Predicted lithium and caesium pentazolates LiN_5 and CsN_5 were successfully synthesized at high-pressure conditions *via* the reaction between a metal or metal azide and nitrogen (Laniel *et al.*, 2018; Steele *et al.*, 2017). Recently, Bykov and co-workers synthesized two compounds containing polymeric nitrogen chains, *viz*. an inclusion compound $ReN_8{\cdot}N_2$ (Bykov *et al.*, 2018*b*) and iron tetranitride, FeN_4 (Bykov *et al.* 2018*a*) *via* the reaction between Fe or Re and nitrogen in a laser-heated diamond anvil cell (DAC). The crystal structures of these compounds were studied at pressures up to 135 GPa by means of single-crystal X-ray diffraction (SCXRD).

The higher the pressures, the more challenging are synthesis and diffraction studies in DACs, even at dedicated high-pressure stations at the 3rd generation synchrotron facilities where the X-ray beam can be focused down to 2–3 μm. First of all, at pressures exceeding 150 GPa, the size of the sample is of only about 10 μm or less, and single-crystalline grains of the reaction product(s) are often of submicron size, which results in a drastic worsening of the signal-to-noise ratio in SCXRD. Additionally, the contribution of parasitic diffraction from the

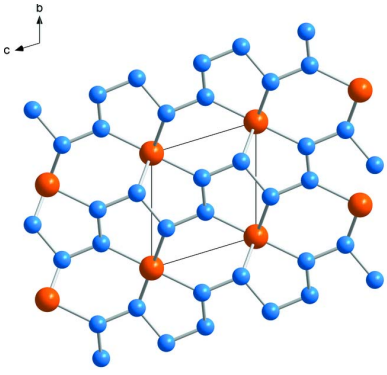

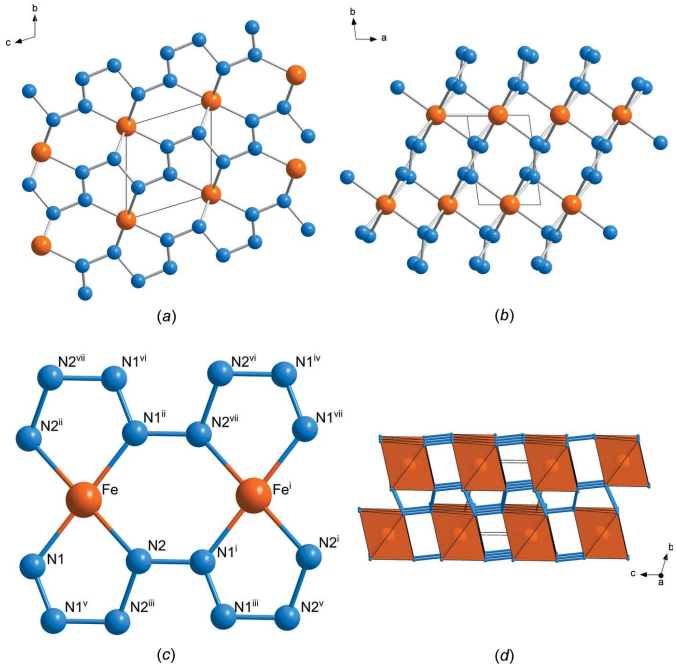

Figure 1
The crystal structure of FeN_4 at 180 GPa. (*a*) and (*b*) Projections of the crystal structure along [100] and [001], respectively. (*c*) A fragment of the crystal structure showing the coordination of Fe atoms. [Symmetry codes: (i) $x, y, 1+z$; (ii) $1-x, -y, -z$; (iii) $-x, 1-y, -z$; (iv) $1+x, 1+y, 2+z$; (v) $-x, -1-y, -1-z$; (vi) $1+x, 1+y, 1+z$; (vii) $1-x, -y, 1-z$; (viii) $1+x, 1+y, z$.] (*d*) The crystal structure of FeN_4 in polyhedral representation.

gasket material increases with pressure because the sample chamber becomes smaller upon compression. Submicron focusing of the X-ray beam, which is possible on some synchrotron beamlines, can provide suitable conditions to collect SCXRD data at multi-megabar pressures. Here we report the synthesis of FeN_4 from the elements at a pressure of about 180 GPa and provide the structure refinement for FeN_4 against SCXRD data at this pressure. The X-ray beam focusing down to 0.3×0.3 μm^2 at the synchrotron beamline ID11 (ESRF, Grenoble, France) allowed us to collect SCXRD data from an FeN_4 grain with linear dimensions of about 0.5 μm.

2. Structural commentary

The crystal structure (Fig. 1*a*,*b*) and the unit-cell volume (Fig. 2) of FeN_4 at 180 GPa are in a good agreement with the structural model for this compound at 135 GPa and its equation of state as reported by Bykov *et al.* (2018*a*). Despite the increased pressure, as a result of the application of the submicron beam focusing, the quality of the SCXRD data collected at 180 GPa turned out to be much better. Thus, the quality of the structure refinement of FeN_4 based on the 180 GPa data set is significantly improved in comparison with that for the 135 GPa data set. This is evident from a comparison of such important refinement indicators such as the data-to-parameter ratio (7.1 *vs* 4.8), $\Delta\rho_{max}/\Delta\rho_{min}$ (0.76/−0.56 *vs* 0.98/−1.09 e Å^{-3}) and $R_1[I>2\sigma(I)]$ (0.040 *vs* 0.064). Furthermore, the precision of the bond lengths and angles is significantly improved (Table 1).

Table 1
Selected bond lengths for FeN_4 at 135 GPa (Bykov *et al.*, 2018*a*) and at 180 GPa (this study).

	135 GPa	180 GPa
Fe—N1	1.73 (2)	1.707 (10)
Fe—N1^{i}	1.73 (2)	1.707 (10)
Fe—N2^{ii}	1.81 (3)	1.783 (14)
Fe—N2^{iii}	1.81 (3)	1.783 (14)
Fe—N2^{iv}	1.78 (3)	1.763 (6)
Fe—N2^{v}	1.78 (3)	1.763 (6)
N1—N1^{vi}	1.29 (5)	1.277 (14)
N1—N2	1.30 (3)	1.298 (8)
N2—N2^{vii}	1.43 (4)	1.37 (3)

Symmetry codes: (i) $-x+1, -y, -z$; (ii) $x+1, y, z+1$; (iii) $-x, -y, -z-1$; (iv) $-x+1, -y, -z-1$; (v) $x, y, z+1$; (vi) $-x, -y-1, -z-1$; (vii) $-x, -y-1, -z-2$.

The Fe1 atom occupies an inversion centre of space-group type $P\overline{1}$ (Wyckoff position 1*d*), while the two nitrogen atoms N1 and N2 occupy general positions (2*i*). The iron atom is coordinated by six nitrogen atoms, forming a distorted octahedron. [FeN_6] octahedra share opposite edges, thus forming infinite chains along [100]. These chains are interconnected through N—N bridges as shown in Fig. 1*d*. The covalently bonded nitrogen atoms form infinite zigzag chains running along [001] (Fig. 1*a*–*c*). The N1 atom has a trigonal–planar coordination, while N2 is tetrahedrally coordinated, suggesting sp^2 and sp^3 hybridization, respectively. In agreement with the study of Bykov *et al.* (2018*a*), the N—N distances increase in the following order d(N1—N1) < d(N1—N2) < d(N2—N2) (Table 1), supporting the conclusion that the N1—N1 bond is a double-bond, while N1—N2 and N2—N2 bonds are single bonds. Therefore, the nitrogen atoms form

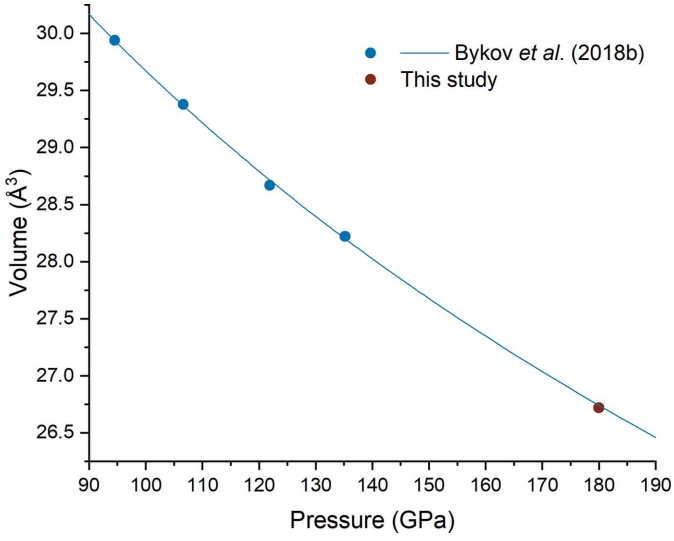

Figure 2
Pressure-dependence of the unit-cell volume of FeN_4. Blue points and the equation of state (blue line) are taken without modification from Bykov *et al.* (2018*a*) [$V_{94.5}$ = 29.94 (4) Å^3, $K_{94.5}$ = 603 (22) GPa, $K'_{94.5}$ = 4.0 (fixed)]. Red point – current study.

Table 2
Pressures for FeN_4 synthesis based on different 3rd order Birch–Murnaghan EoS's of *hcp*-Fe reported in the literature [V_{Fe} = 15.171 (5) Å^3/unit cell].

Reference	V_0 (Å^3)	K (GPa)	K'	Pressure (GPa)
Dewaele *et al.* (2006)	22.468 (24)	165 (fixed)	4.97 (4)	173.5(2.2)
Fei *et al.* (2016)	22.428 (fixed)	172.7(1.4)	4.79 (5)	174.1(1.4)
Sakai *et al.* (2014)	22.18 (20)	179.6(2.2)	4.91 (12)	174.9(2.1)
Mao *et al.* (1990)	22.35 (3)	164.8(3.6)	5.33 (9)	179.8(4.3)
Yamazaki *et al.* (2012)	22.15 (5)	202 (7)	4.5 (2)	181.0(5.6)
Dubrovinsky *et al.* (2000)	22.35 (3)	155.6(3.5)	5.81 (6)	183.7(4.8)
Garai *et al.* (2011)	22.33 (3)	164 (2)	5.52 (5)	183.9(2.5)
Boehler *et al.* (2008)	22.46 (4)	160 (6)	5.6 (2)	187.5(8.2)

catena-poly[tetraz-1-ene-1,4-diyl] anions $[–N{=}N–N{=}N–]_\infty^{2–}$.

The key parameters for the synthesis of polynitrides are pressure–temperature conditions and the choice of metal and/or nitrogen precursors. High temperatures and pressures are required to overcome the kinetic barrier for breaking the triple N≡N bond, to increase the chemical potential of nitrogen and to stabilize the reaction products (Sun *et al.*, 2017). It is known that increasing pressure allows compounds with higher nitrogen content to be obtained, *e.g.* for the Fe—N system Fe_xN (x = 2–8) can be synthesized at ambient and low pressures (Ertl *et al.* 1979), FeN at 12 GPa (Clark *et al.*, 2017), FeN_2 at 60 GPa, and FeN_4 at 106 GPa (Bykov *et al.*, 2018*a*). Interestingly, at a given pressure, different metals stabilize different types of nitrogen networks. For example, $ReN_8{\cdot}N_2$ synthesized at 106 GPa contains polydiazene chains $[–N{=}N–]_\infty$ (Bykov *et al.*, 2018*b*), whereas alkali metals form pentazolate salts at even lower pressures (Laniel *et al.*, 2018; Steele *et al.*, 2017), *i.e.* the type of metal, the variety of its oxidation states, and its ionic radius play an important role in the chemistry of the nitrogen network. The current study shows that FeN_4 can be synthesized in a broad pressure range from 106 to 180 GPa. Such an extended stability range for this compound may be related to the favourable sixfold coordination of Fe. On one hand, it perfectly matches the 18 e^- rule (Bykov *et al.*, 2018*a*), and on the other hand, for the Fe—N system coordination number 6 is geometrically preferable. Further systematic studies of various metal polynitrides will allow empirical rules for the design of novel materials at different pressure and temperature conditions to be formulated.

3. Synthesis and crystallization

A piece of iron powder (Sigma Aldrich, 99.99%) was loaded inside a sample chamber of a BX90-type diamond anvil cell equipped with double-bevelled Boehler–Almax type diamonds (culet diameter 40 µm). Nitrogen was used as a pressure-transmitting medium and as a reagent for the synthesis. The sample was compressed up to 180 GPa and laser-heated from both sides up to 2700 (200) K. The pressure was determined using the equation of state (EoS) of *hcp*-iron. As there are several equations of state of iron in the literature (Table 2), for a given unit-cell volume of iron V_{Fe} = 15.171 (5) Å^3 one can get slightly different pressures in the range 173.5 to 187.5 GPa with an average of 179.8(5.2) GPa. Taking into account this uncertainty in the pressure determination, we accepted the rounded value of 180 GPa.

In order to locate the FeN_4 grain in the sample chamber we used the following strategy: we collected 27 × 27 = 729 still images with the exposure time of 6 s. Before taking the next image, either the horizontal or vertical motor was moved by 0.5 µm, allowing a 13 × 13 µm^2 X-ray diffraction map of the sample chamber to be built up (Fig. 3). The images were then analyzed with *XDI* software (Hrubiak, 2017).

4. Refinement

Crystal data, data collection details and structure refinement details are summarized in Table 3. We have used the same non-reduced unit-cell setting and the structure model of FeN_4 at 135 GPa (Bykov *et al.*, 2018*a*) for refinement of the crystal

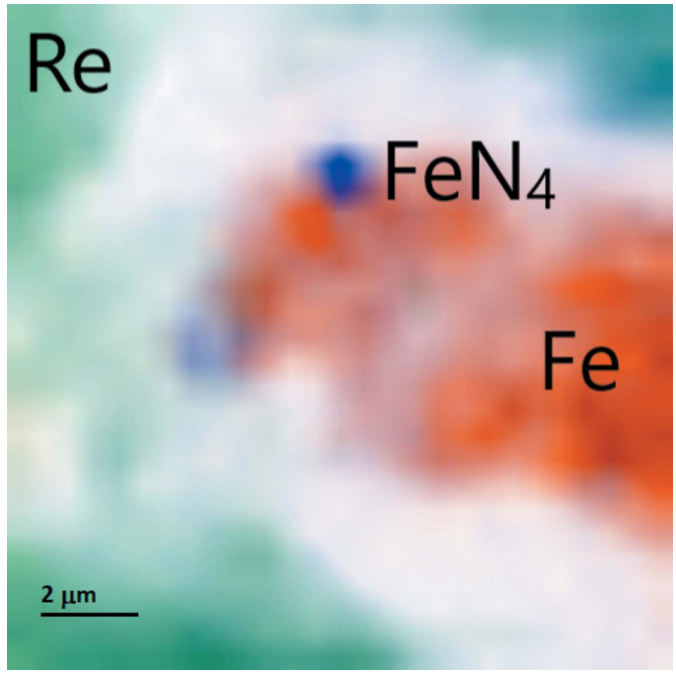

Figure 3
X-ray diffraction imaging of the sample chamber at 180 GPa. The colour intensity is proportional to the intensity of the following reflections: the (100) reflection of Re for the green region; the (101) reflection of Fe for the orange region; the sum of the (101), (1$\bar{1}$1), (0 0 2), and ($\bar{1}$$\bar{1}$2) reflections of FeN_4 for the blue region.

Table 3
Experimental details.

Crystal data	
Chemical formula	FeN_4
M_r	111.89
Crystal system, space group	Triclinic, $P\overline{1}$
Temperature (K)	293
a, b, c (Å)	2.4473 (10), 3.4688 (14), 3.5144 (13)
α, β, γ (°)	105.22 (4), 110.60 (4), 91.39 (3)
V (Å^3)	26.72 (2)
Z	1
Radiation type	Synchrotron, λ = 0.30996 Å
μ (mm^{-1})	1.33
Crystal size (mm)	0.0005 × 0.0005 × 0.0005
Data collection	
Diffractometer	ID11 @ ESRF
Absorption correction	Multi-scan (*ABSPACK*; Oxford Diffraction, 2005)
T_{min}, T_{max}	0.967, 1.000
No. of measured, independent and observed [$I > 2\sigma(I)$] reflections	117, 71, 70
R_{int}	0.020
(sin $\theta/\lambda)_{max}$ (Å^{-1})	0.901
Refinement	
$R[F^2 > 2\sigma(F^2)]$, $wR(F^2)$, S	0.040, 0.082, 1.18
No. of reflections	71
No. of parameters	10
$\Delta\rho_{max}$, $\Delta\rho_{min}$ (e Å^{-3})	0.76, −0.56

Computer programs: *CrysAlis PRO* (Rigaku OD, 2018), *SHELXT* (Sheldrick, 2015*a*), *SHELXL2014* (Sheldrick, 2015*b*) and *OLEX2* (Dolomanov *et al.*, 2009).

structure of FeN_4 at 180 GPa. As a result of the limited angular range caused by the laser-heated DAC and the very small crystal size, the resolution of the data set was not sufficient to refine the atoms with anisotropic displacement parameters. Hence they were refined with isotropic displacement parameters only.

Acknowledgements

The diffraction experiments were performed on beamline ID11 at the European Synchrotron Radiation Facility (ESRF), Grenoble, France.

References

Boehler, R., Santamaría-Pérez, D., Errandonea, D. & Mezouar, M. (2008). *J. Phys. Conf. Ser.* **121**, 022018.
Bykov, M., Bykova, E., Aprilis, G., Glazyrin, K., Koemets, E., Chuvashova, I., Kupenko, I., McCammon, C., Mezouar, M., Prakapenka, V., Liermann, H.-P., Tasnádi, F., Ponomareva, A. V., Abrikosov, I. A., Dubrovinskaia, N. & Dubrovinsky, L. (2018*a*). *Nat. Commun.* **9**, 2756.
Bykov, M., Bykova, E., Koemets, E., Fedotenko, T., Aprilis, G., Glazyrin, K., Liermann, H.-P., Ponomareva, A. V., Tidholm, J., Tasnádi, F., Abrikosov, I. A., Dubrovinskaia, N. & Dubrovinsky, L. (2018*b*). *Angew. Chem. Int. Ed.* **57**, 9048–9053.
Clark, W. P., Steinberg, S., Dronskowski, R., McCammon, C., Kupenko, I., Bykov, M., Dubrovinsky, L., Akselrud, L. G., Schwarz, U. & Niewa, R. (2017). *Angew. Chem. Int. Ed.* **56**, 7302–7306.
Dewaele, A., Loubeyre, P., Occelli, F., Mezouar, M., Dorogokupets, P. I. & Torrent, M. (2006). *Phys. Rev. Lett.* **97**, 215504.
Dolomanov, O. V., Bourhis, L. J., Gildea, R. J., Howard, J. A. K. & Puschmann, H. (2009). *J. Appl. Cryst.* **42**, 339–341.
Dubrovinsky, L., Saxena, S., Tutti, F., Rekhi, S. & LeBehan, T. (2000). *Phys. Rev. Lett.* **84**, 1720–1723.
Ertl, G., Huber, M. & Thiele, N. (1979). *Z. Naturforsch. Teil A*, **34**, 30–39.
Fei, Y., Murphy, C., Shibazaki, Y., Shahar, A. & Huang, H. (2016). *Geophys. Res. Lett.* **43**, 6837–6843.
Garai, J., Chen, J. & Telekes, G. (2011). *Am. Mineral.* **96**, 828–832.
Hrubiak, R. (2017). *XDI*. High Pressure Collaborative Access Team, Geophysical Laboratory, Carnegie Institution of Washington, Argonne, Illinois 60439, USA.
Laniel, D., Weck, G., Gaiffe, G., Garbarino, G. & Loubeyre, P. (2018). *J. Phys. Chem. Lett.* **9**, 1600–1604.
Mao, H. K., Wu, Y., Chen, L. C., Shu, J. F. & Jephcoat, A. P. (1990). *J. Geophys. Res.* **95**, 21737.
Oxford Diffraction (2005). *ABSPACK*. Oxford Diffraction Ltd, Abingdon, England.
Rigaku OD (2018). *CrysAlis PRO*. Rigaku Oxford Diffraction, Yarnton, UK.
Sakai, T., Takahashi, S., Nishitani, N., Mashino, I., Ohtani, E. & Hirao, N. (2014). *Phys. Earth Planet. Inter.* **228**, 114–126.
Sheldrick, G. M. (2015*a*). *Acta Cryst.* A**71**, 3–8.
Sheldrick, G. M. (2015*b*). *Acta Cryst.* C**71**, 3–8.
Steele, B. A. & Oleynik, I. I. (2016). *Chem. Phys. Lett.* **643**, 21–26.
Steele, B. A. & Oleynik, I. I. (2017). *J. Phys. Chem. A*, **121**, 8955–8961.
Steele, B. A., Stavrou, E., Crowhurst, J. C., Zaug, J. M., Prakapenka, V. B. & Oleynik, I. I. (2017). *Chem. Mater.* **29**, 735–741.
Sun, W., Holder, A., Orvañanos, B., Arca, E., Zakutayev, A., Lany, S. & Ceder, G. (2017). *Chem. Mater.* **29**, 6936–6946.
Xia, K., Gao, H., Liu, C., Yuan, J., Sun, J., Wang, H.-T. & Xing, D. (2018). *Sci. Bull.* **63**, 817–824.
Yamazaki, D., Ito, E., Yoshino, T., Yoneda, A., Guo, X., Zhang, B., Sun, W., Shimojuku, A., Tsujino, N., Kunimoto, T., Higo, Y. & Funakoshi, K. (2012). *Geophys. Res. Lett.* **39**, l20308.
Zhang, S., Zhao, Z., Liu, L. & Yang, G. (2017). *J. Power Sources*, **365**, 155–161.

supporting information

Acta Cryst. (2018). E**74**, 1392-1395 [https://doi.org/10.1107/S2056989018012161]

Synthesis of FeN_4 at 180 GPa and its crystal structure from a submicron-sized grain

Maxim Bykov, Saiana Khandarkhaeva, Timofey Fedotenko, Pavel Sedmak, Natalia Dubrovinskaia and Leonid Dubrovinsky

Computing details

Data collection: *CrysAlis PRO* (Rigaku OD, 2018); cell refinement: *CrysAlis PRO* (Rigaku OD, 2018); data reduction: *CrysAlis PRO* (Rigaku OD, 2018); program(s) used to solve structure: SHELXT (Sheldrick, 2015*a*); program(s) used to refine structure: *SHELXL2014* (Sheldrick, 2015*b*); molecular graphics: *OLEX2* (Dolomanov *et al.*, 2009); software used to prepare material for publication: *OLEX2* (Dolomanov *et al.*, 2009).

Iron tetranitride

Crystal data

FeN_4
M_r = 111.89
Triclinic, $P\overline{1}$
a = 2.4473 (10) Å
b = 3.4688 (14) Å
c = 3.5144 (13) Å
α = 105.22 (4)°
β = 110.60 (4)°
γ = 91.39 (3)°
V = 26.72 (2) Å^3
Z = 1
$F(000)$ = 54
D_x = 6.953 Mg m^{-3}
Synchrotron radiation, λ = 0.30996 Å
Cell parameters from 68 reflections
θ = 2.8–16.1°
μ = 1.33 mm^{-1}
T = 293 K
Irregular, black
0.001 × 0.001 × 0.001 mm

Data collection

ID11 @ ESRF diffractometer
Radiation source: synchrotron
Synchrotron monochromator
ω scans
Absorption correction: multi-scan (*ABSPACK*; Oxford Diffraction, 2005)
T_{min} = 0.967, T_{max} = 1.000
117 measured reflections
71 independent reflections
70 reflections with $I > 2\sigma(I)$
R_{int} = 0.020
θ_{max} = 16.2°, θ_{min} = 2.8°
h = −3→3
k = −5→4
l = −6→5

Refinement

Refinement on F^2
Least-squares matrix: full
$R[F^2 > 2\sigma(F^2)]$ = 0.040
$wR(F^2)$ = 0.082
S = 1.18
71 reflections
10 parameters
0 restraints
Primary atom site location: dual
$w = 1/[\sigma^2(F_o^2) + (0.0282P)^2 + 0.3122P]$ where $P = (F_o^2 + 2F_c^2)/3$
$(\Delta/\sigma)_{max} < 0.001$
$\Delta\rho_{max}$ = 0.76 e Å^{-3}
$\Delta\rho_{min}$ = −0.56 e Å^{-3}

Special details

Geometry. All esds (except the esd in the dihedral angle between two l.s. planes) are estimated using the full covariance matrix. The cell esds are taken into account individually in the estimation of esds in distances, angles and torsion angles; correlations between esds in cell parameters are only used when they are defined by crystal symmetry. An approximate (isotropic) treatment of cell esds is used for estimating esds involving l.s. planes.

Fractional atomic coordinates and isotropic or equivalent isotropic displacement parameters (Å²)

	x	*y*	*z*	U_{iso}*/U_{eq}
Fe	0.5000	0.0000	0.0000	0.0072 (4)*
N1	0.163 (4)	−0.346 (4)	−0.485 (2)	0.0066 (10)*
N2	0.065 (3)	−0.309 (4)	−0.861 (2)	0.0068 (10)*

Geometric parameters (Å, º)

Fe—Fe^{i}	2.4473 (10)	Fe—N2^{vii}	1.763 (6)
Fe—Fe^{ii}	2.4473 (10)	N1—N1^{viii}	1.277 (14)
Fe—N1	1.707 (10)	N1—N2	1.298 (8)
Fe—N1^{iii}	1.707 (10)	N2—Fe^{ix}	1.763 (6)
Fe—N2^{iv}	1.783 (14)	N2—Fe^{x}	1.783 (14)
Fe—N2^{v}	1.783 (14)	N2—N2^{xi}	1.37 (3)
Fe—N2^{vi}	1.763 (6)		
Fe^{i}—Fe—Fe^{ii}	180.0	N2^{vii}—Fe—Fe^{ii}	46.7 (5)
N1—Fe—Fe^{i}	96.6 (4)	N2^{iv}—Fe—Fe^{ii}	133.98 (18)
N1^{iii}—Fe—Fe^{ii}	96.6 (4)	N2^{iv}—Fe—Fe^{i}	46.02 (18)
N1—Fe—Fe^{ii}	83.4 (4)	N2^{vii}—Fe—N2^{v}	92.7 (5)
N1^{iii}—Fe—Fe^{i}	83.4 (4)	N2^{vi}—Fe—N2^{v}	87.3 (5)
N1^{iii}—Fe—N1	180.0	N2^{v}—Fe—N2^{iv}	180.0 (7)
N1—Fe—N2^{vii}	81.3 (4)	N2^{vii}—Fe—N2^{iv}	87.3 (5)
N1^{iii}—Fe—N2^{vii}	98.7 (4)	N2^{vi}—Fe—N2^{iv}	92.7 (5)
N1^{iii}—Fe—N2^{vi}	81.3 (4)	N2^{vi}—Fe—N2^{vii}	180.0
N1—Fe—N2^{vi}	98.7 (4)	N1^{viii}—N1—Fe	118.9 (9)
N1—Fe—N2^{iv}	90.5 (5)	N1^{viii}—N1—N2	109.6 (9)
N1—Fe—N2^{v}	89.5 (5)	N2—N1—Fe	129.4 (9)
N1^{iii}—Fe—N2^{v}	90.5 (5)	Fe^{ix}—N2—Fe^{x}	87.3 (5)
N1^{iii}—Fe—N2^{iv}	89.5 (5)	N1—N2—Fe^{x}	110.9 (12)
N2^{vi}—Fe—Fe^{i}	46.7 (5)	N1—N2—Fe^{ix}	126.9 (5)
N2^{vi}—Fe—Fe^{ii}	133.3 (5)	N1—N2—N2^{xi}	107.6 (12)
N2^{vii}—Fe—Fe^{i}	133.3 (5)	N2^{xi}—N2—Fe^{x}	113.1 (6)
N2^{v}—Fe—Fe^{ii}	46.02 (18)	N2^{xi}—N2—Fe^{ix}	109.9 (9)
N2^{v}—Fe—Fe^{i}	133.98 (18)		

Symmetry codes: (i) *x*+1, *y*, *z*; (ii) *x*−1, *y*, *z*; (iii) −*x*+1, −*y*, −*z*; (iv) *x*+1, *y*, *z*+1; (v) −*x*, −*y*, −*z*−1; (vi) −*x*+1, −*y*, −*z*−1; (vii) *x*, *y*, *z*+1; (viii) −*x*, −*y*−1, −*z*−1; (ix) *x*, *y*, *z*−1; (x) *x*−1, *y*, *z*−1; (xi) −*x*, −*y*−1, −*z*−2.